Observable Two-Step Nucleation Mechanism in Solid-State Formation of Tungsten Carbide

Linfeng Fei,[1] Xianglai Gan,[2] Sheung Mei Ng,[1] Hui Wang,[1,2] Ming Xu,[1] Wei Lu,[1] Yanchun Zhou,[3] Chi Wah Leung,[1] Chee-Leung Mak,[1] and Yu Wang[2]**

[1] Department of Applied Physics, The Hong Kong Polytechnic University, Hong Kong SAR, China

[2] School of Materials Science and Engineering, Nanchang University, Nanchang, Jiangxi 330031, China

[3] Science and Technology on Advanced Functional Composite Laboratory, Aerospace Research Institute of Materials & Processing Technology, Beijing 100076, China

* Correspondence should be addressed to: apaclmak@polyu.edu.hk (C.-L.M.) or wangyu@ncu.edu.cn (Y.W.).

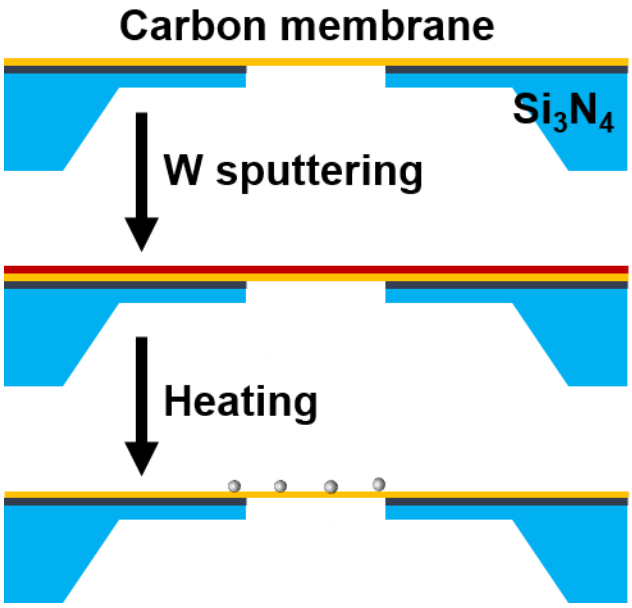

Figure S1. Schematic illustration of the experimental design on observation of solid-state nucleation dynamics from W/C heterostructure. The interfacial reaction of tungsten and carbon during vacuum heating leads to the formation of tungsten carbide nanoparticles from amorphous precursor.

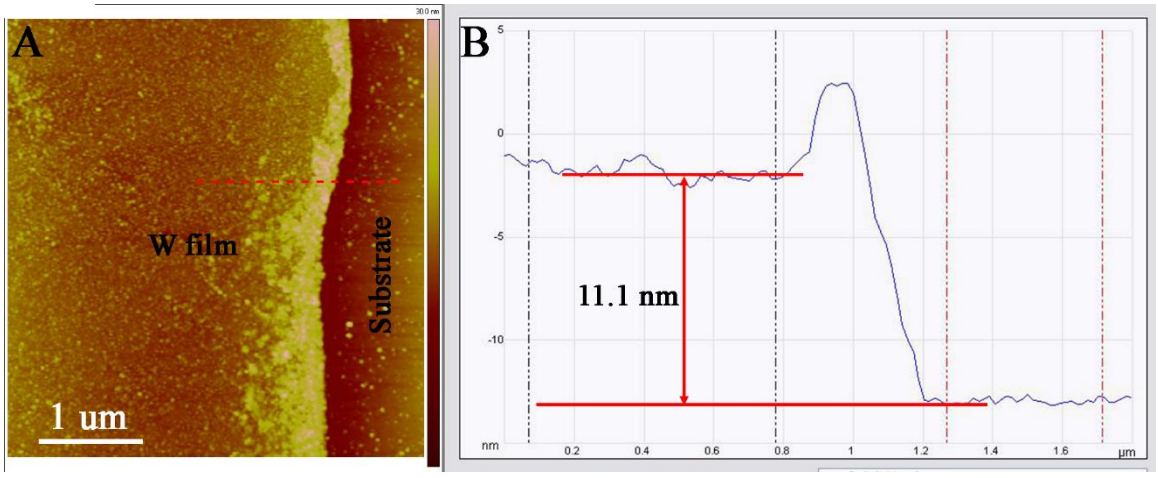

Figure S2. AFM characterization of the thickness of amorphous W film. (A) The AFM topographic image across the edge part of the W film. (B) The height profile for the red dashed line in (A), showing the average thickness of ~ 11 nm for the W film. The AFM sample is prepared by depositing metal films on substrate followed by lift-off process to create a step for measurement.

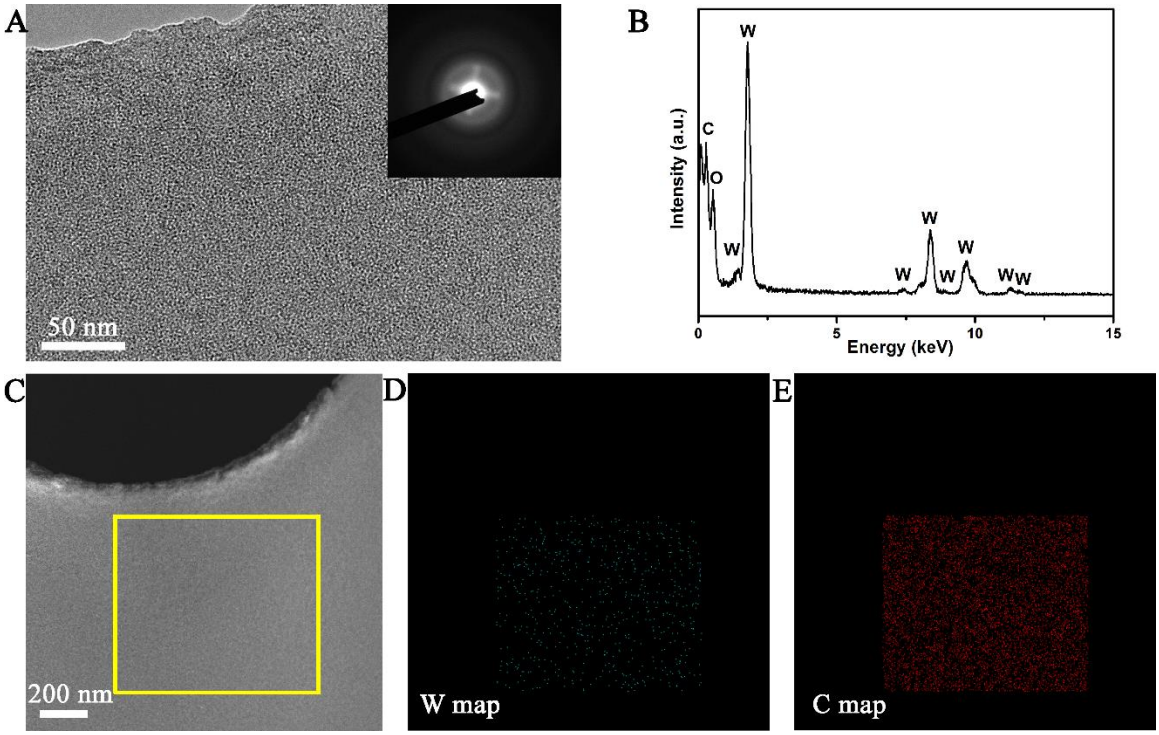

Figure S3. TEM analysis of the W/C heterostructure. (A) The typical TEM image of the W on C film. The inset is the SAED pattern from the region, showing the amorphous nature of the heterostructure. (B) The corresponding EDS spectrum for (A). (C) The HAADF-STEM image of the W/C heterostructure, and the associated elemental maps for (D) tungsten and (E) carbon from the yellow rectangle region of (C).

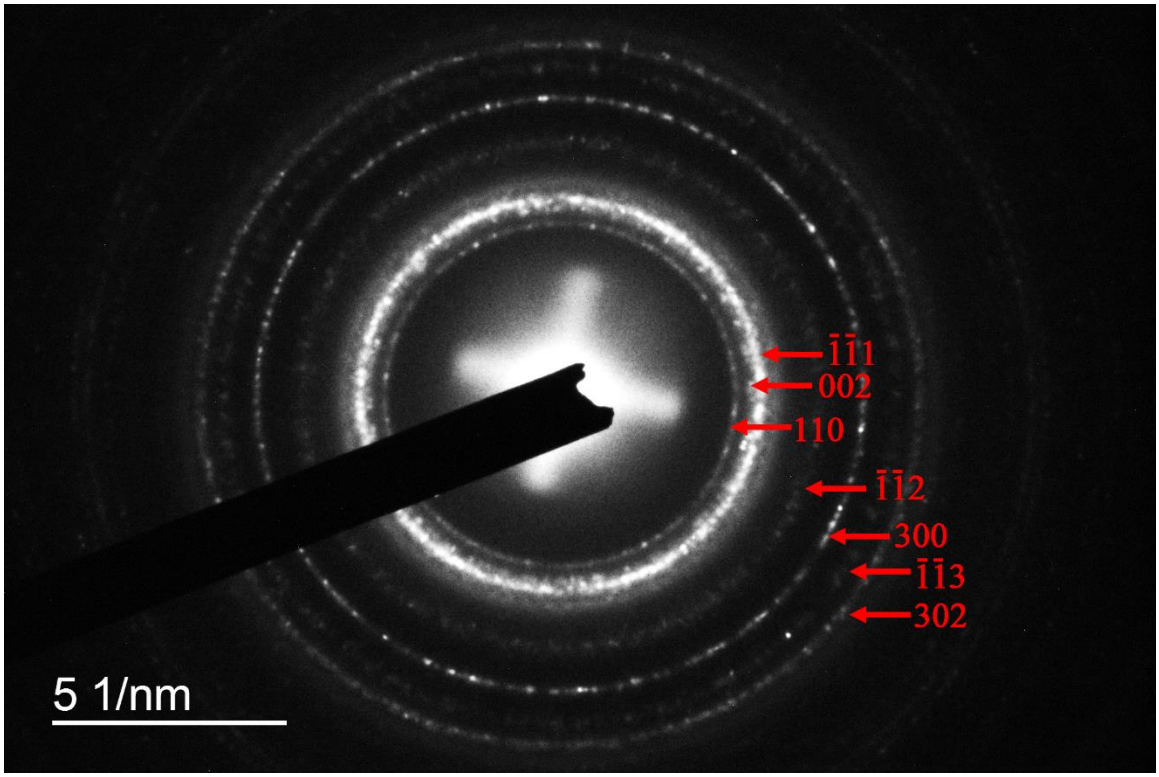

Figure S4. The phase identification from SAED pattern. The full assignment of SAED pattern for hexagonal W_2C obtained during annealing at 1200 ^oC.

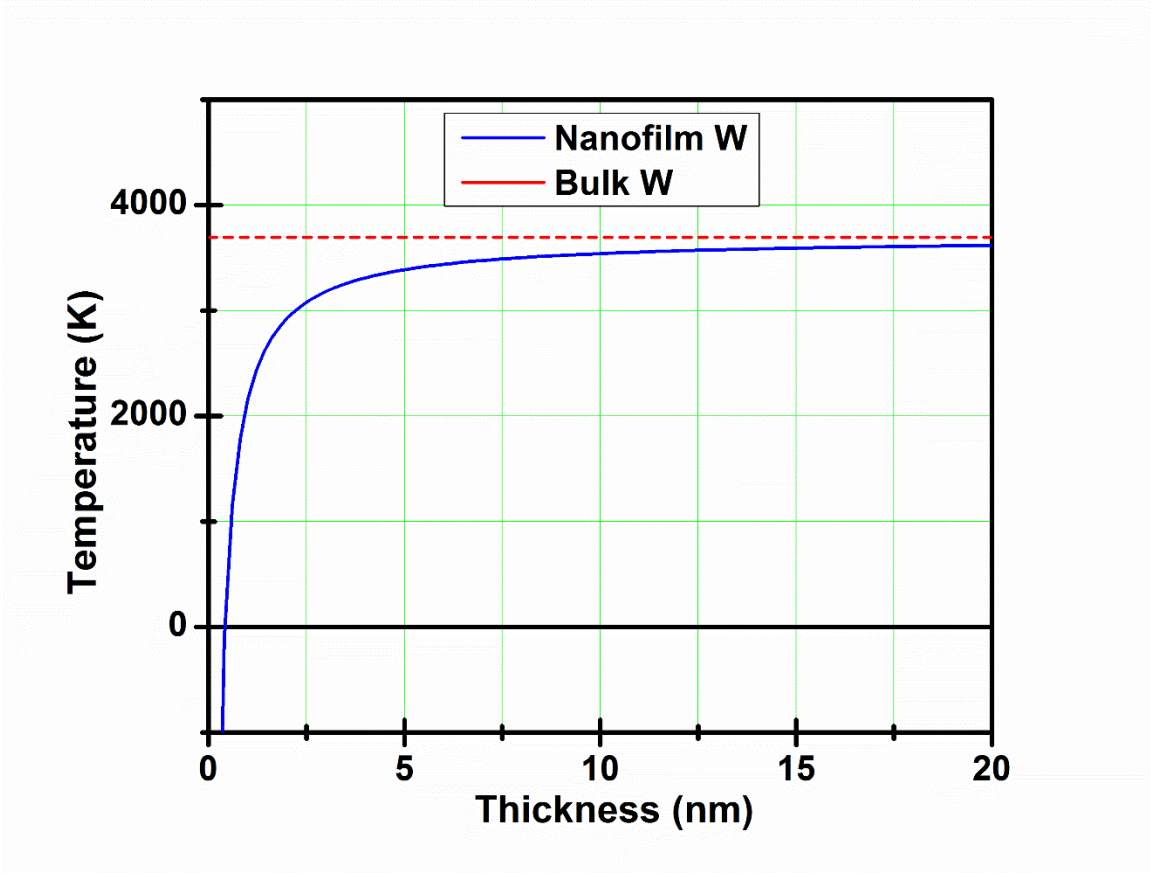

Figure S5. The calculated profile of melting temperature *v.s.* thickness of W film (the blue line). The referenced bulk W material has a melting point of 3695 K (3422 °C, the red dashed line), while the W film of 10 nm thickness has a melting point of 3540 K (3267 °C).

We estimate the melting temperature of the ultra-thin W film, in order to guarantee the experimental phenomena in **Figure 1** is resulted from the interfacial reaction of W and C, and not the melting of W nanofilm.

Xie *et al.* have developed a model,[1,2] concerning the molar cohesive energy of nanostructures and its linear relation with melting point, which suggests (for nanofilms):

$$T_n = T_0\left(1 - \frac{3r}{D}\right)$$

In which T_n is the melting temperature of the nanofilm, T_0 is the transition temperature of the corresponding bulk material, and *r* is the minimal possible thickness of the material. Therefore, T_n is plotted over the thickness *D* of W nanofilm in the above figure (the blue line). The melting temperature of 10 nm W film (3267 ^{o}C) is far higher than the experimental temperature region (up to 1200 ^{o}C); which means that, the experimental phenomena in **Figure 1** is indeed resulted from the interfacial reaction of W and C in our work.

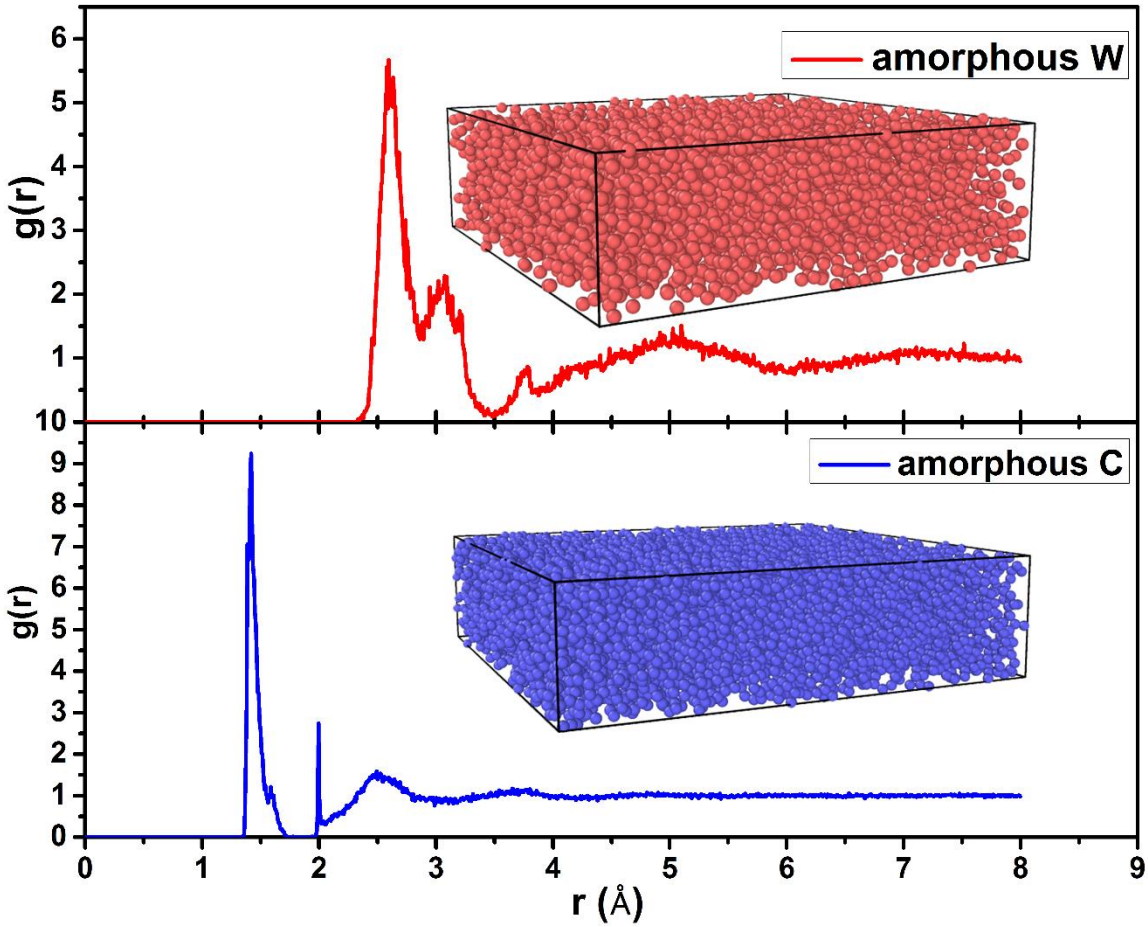

Figure S6. The radial distribution functions of the W and C structures used in the MD simulations, showing their distinct amorphous characteristics. The insets are their corresponding structures.

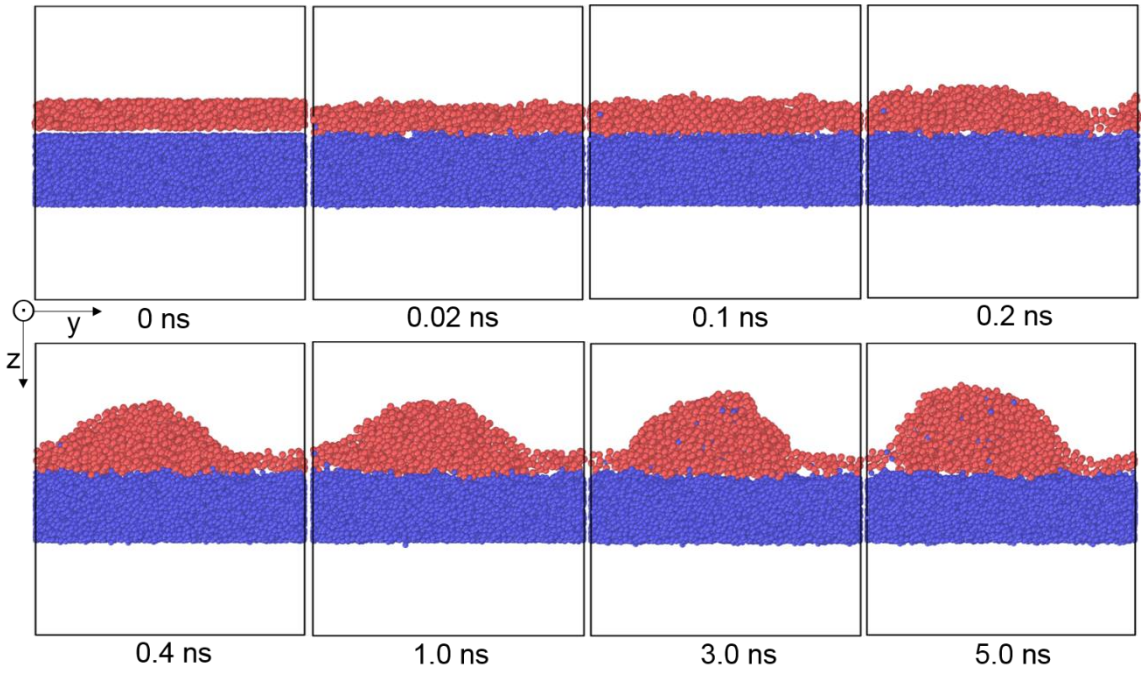

Figure S7. MD simulations of the proposed two-step nucleation. The side-view dynamics of microstructural evolution for the amorphous W/C heterostructure (composed of a 7.4 Å thick amorphous W film and an 18.99 Å thick amorphous C film) *V.S.* annealing time. The red and blue spheres represent W and C atoms, respectively. See also **Figure 2** and **Supplementary Movie S3** for the plane view.

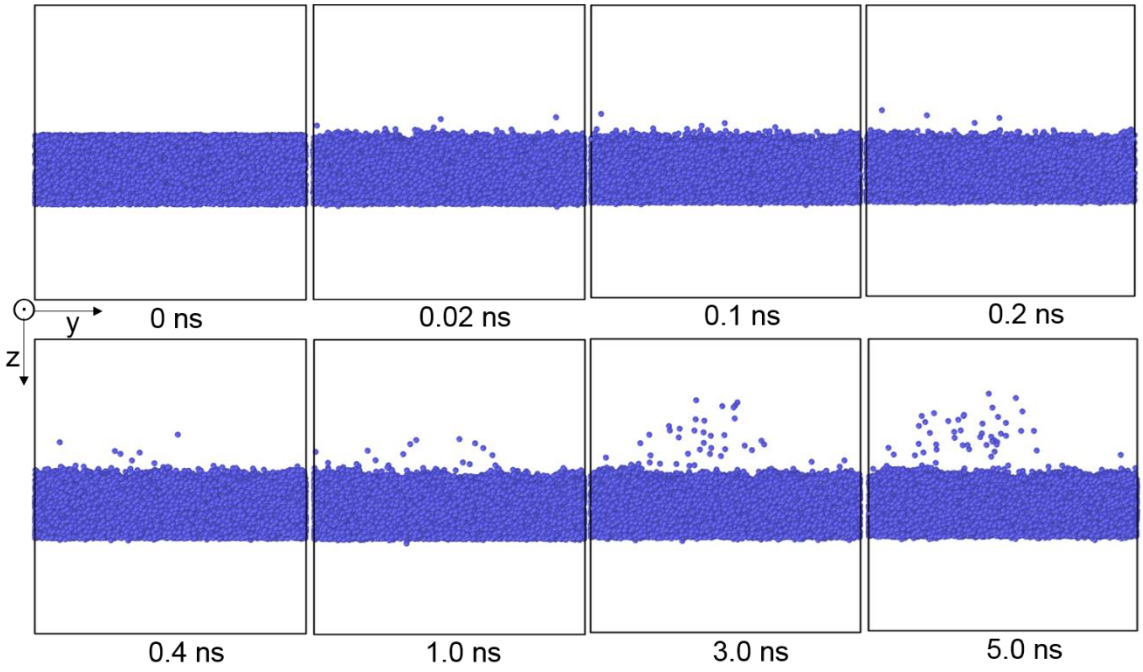

Figure S8. MD simulations of the proposed two-step nucleation. The side-view dynamics of microstructural evolution for the amorphous W/C heterostructure (composed of a 7.4 Å thick amorphous W film and an 18.99 Å thick amorphous C film) *V.S.* annealing time. Only C atoms (as blue spheres) are shown in this figure to clarify the continuous invasion of C into W during annealing. See also **Figure 2** and **Supplementary Movie S3** for the plane view.

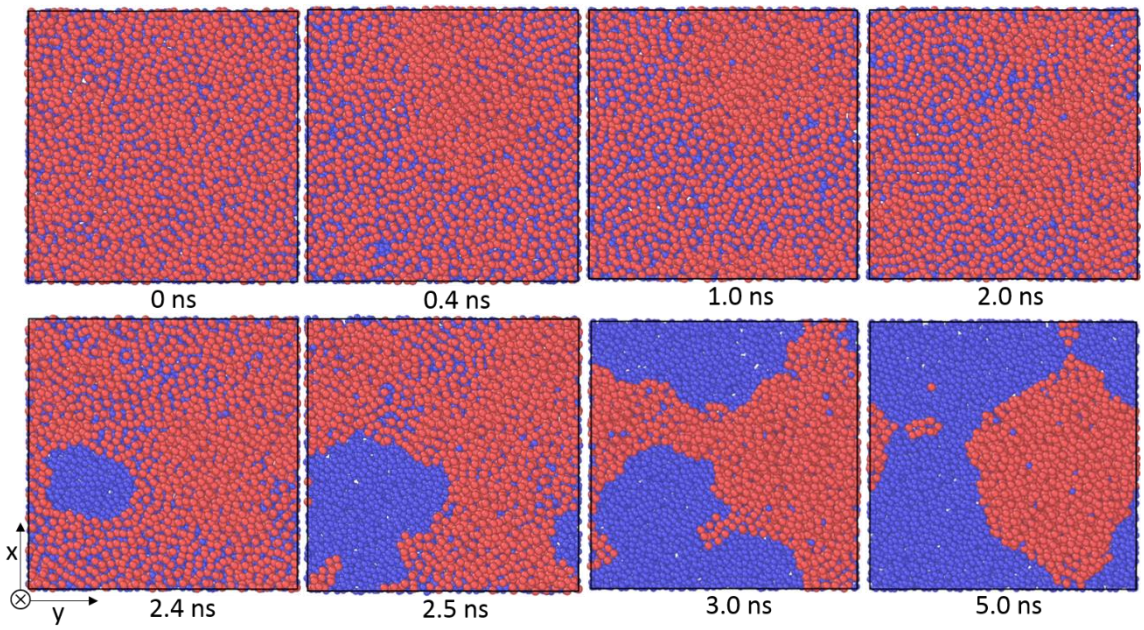

Figure S9. MD simulations of the proposed two-step nucleation. The plan-view dynamics of microstructural evolution for the amorphous W/C heterostructure (composed of a 6.32 Å thick amorphous W film and an 18.9 Å thick amorphous C film, group 1 in **Table S2**) *V.S.* annealing time. The red and blue spheres represent W and C atoms, respectively.

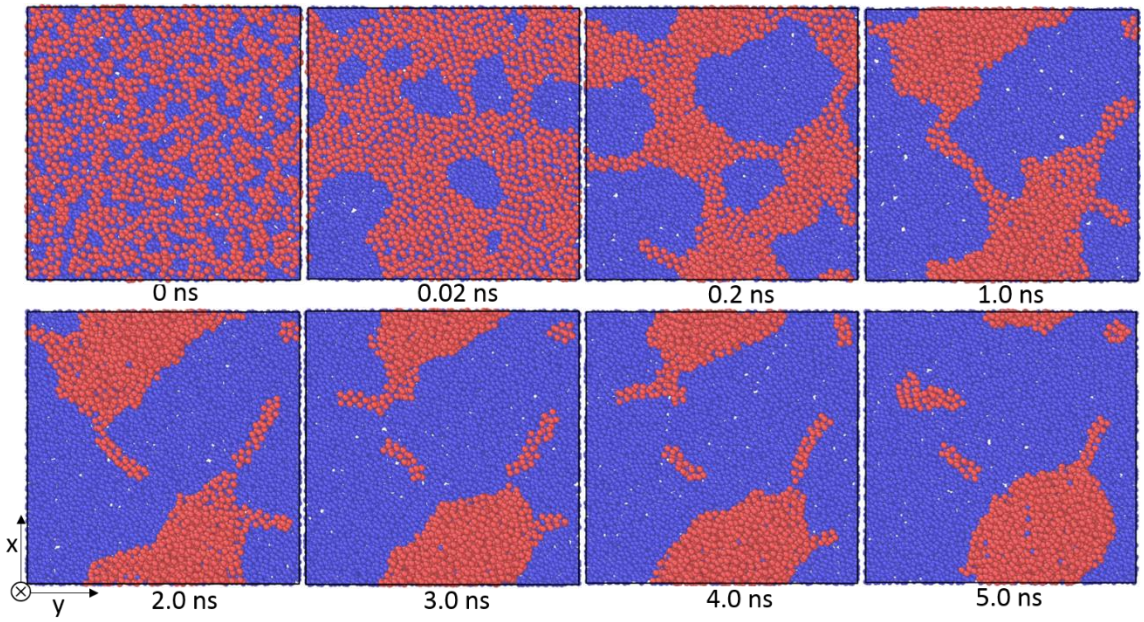

Figure S10. MD simulations of the proposed two-step nucleation. The plan-view dynamics of microstructural evolution for the amorphous W/C heterostructure (composed of a 12 Å thick amorphous W film and an 18.9 Å thick amorphous C film, group 3 in **Table S2**) *V.S.* annealing time. The red and blue spheres represent W and C atoms, respectively.

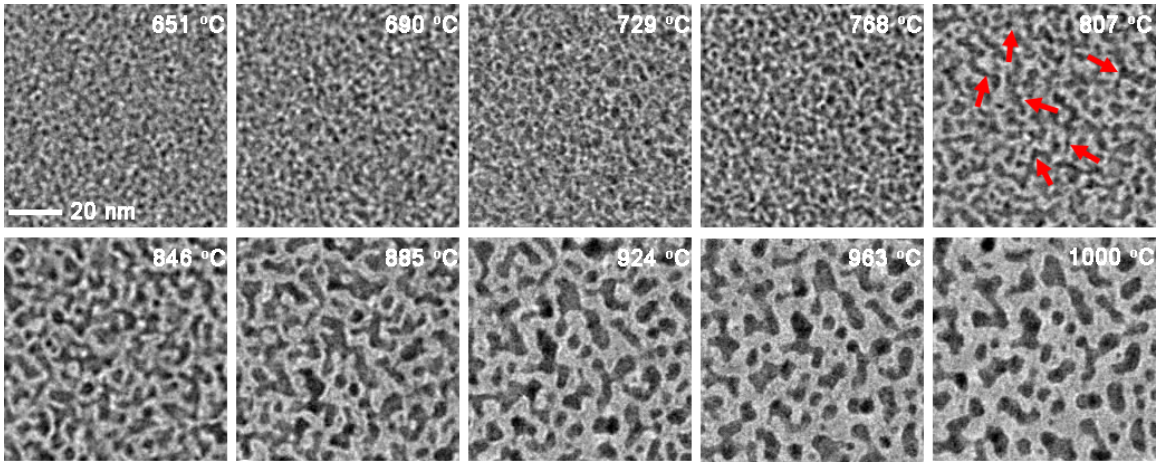

Figure S11. Representative magnified TEM micrographs show details of the spinodal process during temperature ramping. The corresponding reaction temperatures are indicated on the top-right corner of each frame. A few nucleation points can be identified at ~ 800 °C, indicated by the red arrows. The scale bar in the first frame applies to the subsequent ones.

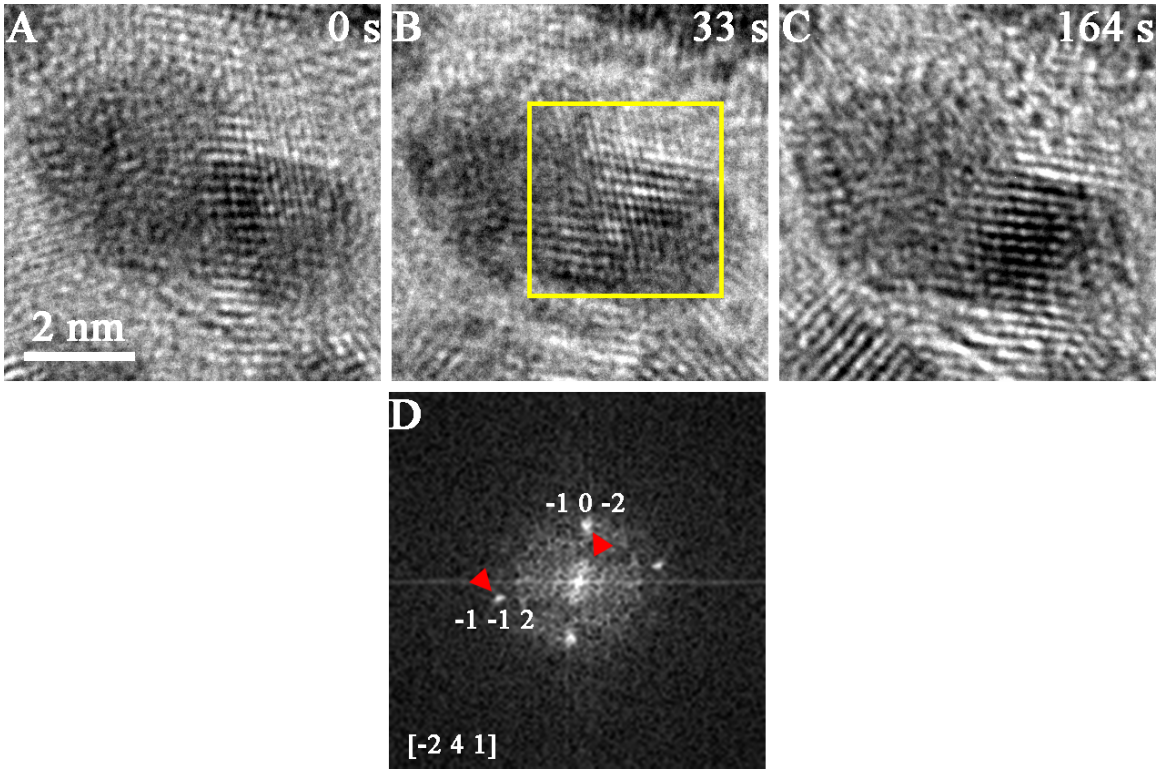

Figure S12. Another crystallization event of a W_2C nanoparticle. (A - C) High-resolution snapshots on expanding of crystallization in an irregular nanoparticle. Time listed for all figures is relative to the first frame. The scale bar in (A) applies to (B) and (C). (D) The FFT pattern of the area of nucleus in (B), marked by the yellow square.

We recorded another nucleation event within a SSAI, which also shows similar nucleation dynamics as that of **Figure 3**; including single nucleus emerged from a concave angle, and the nucleus grew by consuming the amorphous WC_x matrix with a steady crystalline orientation.

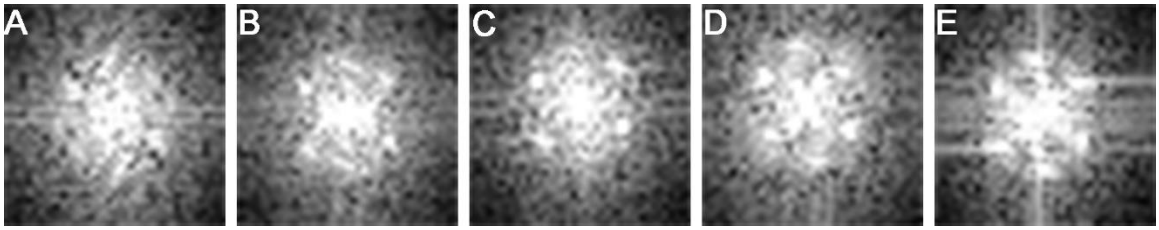

Figure S13. The evolution of FFT patterns a small particle upon annealed at 700 °C. These FFT patterns are associated with the HRTEM micrographs in **Figure 4** (a - e).

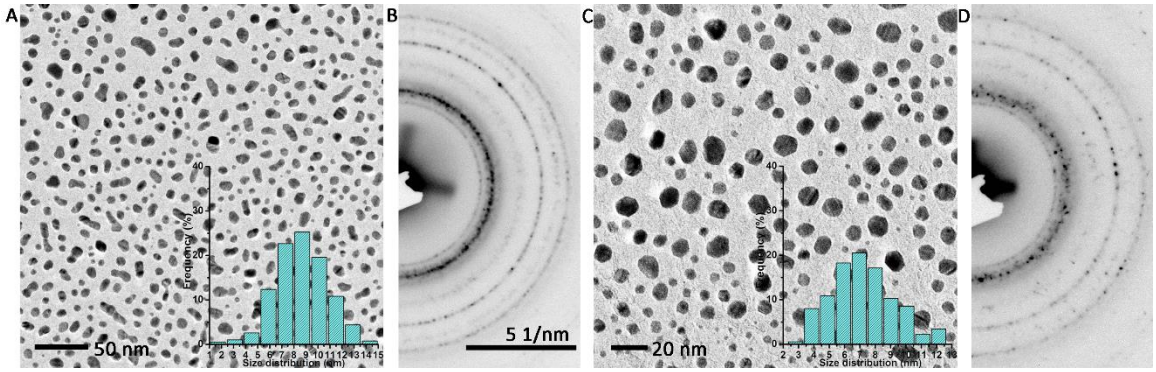

Figure S14. Evaluation of electron beam effect on nucleation mechanism in this work. The bright-field TEM images and the corresponding SAED diffractograms from (A - B) an irradiated area and (C - D) an unirradiated area after annealed at 1200 ^{o}C for 20 minutes, respectively. The assignment of (B) and (D) refers to **Figure S4**. The insets in (A) and (C) are corresponding statistical histograms for particle size distribution. The scale bar in (B) also applies to (D). The two groups of nanoparticles show similar morphology, size distribution and crystallinity, suggesting negligible electron beam effect throughout this experiment.

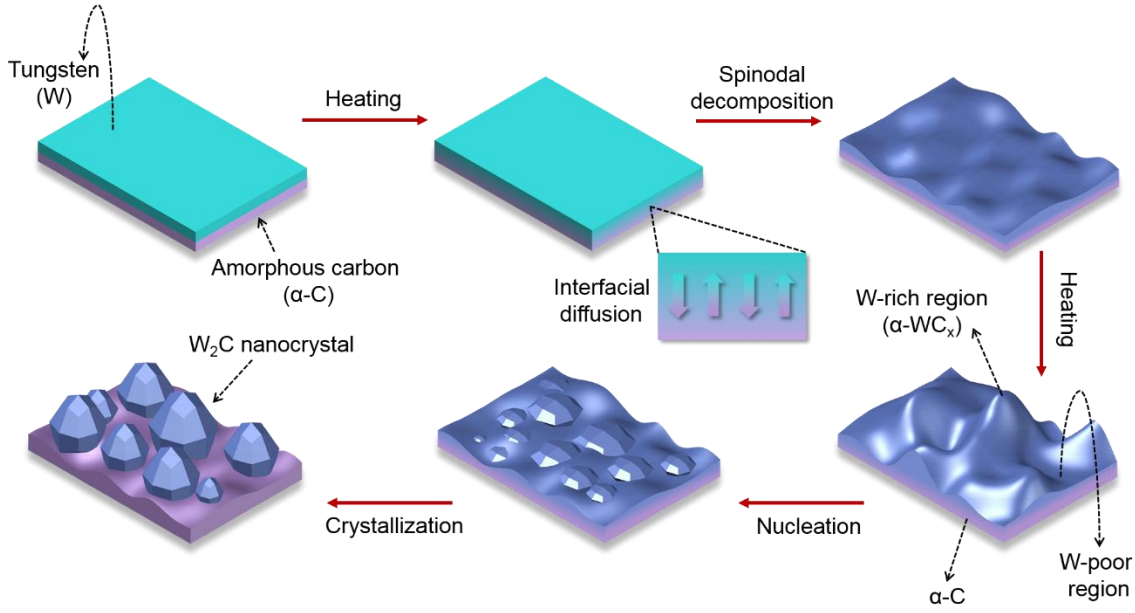

Figure S15. Schematic illustration of the structural evolution driven by solid-state reaction from W/C heterostructure. Upon heating, the 2D amorphous tungsten/carbon structure begins interfacial diffusion which then causes spinodal decomposition of the upper WC_x layer to give isolated SSAIs. Nuclei precipitate within SSAIs and then develop themselves, leading to the formation of W_2C nanocrystals.

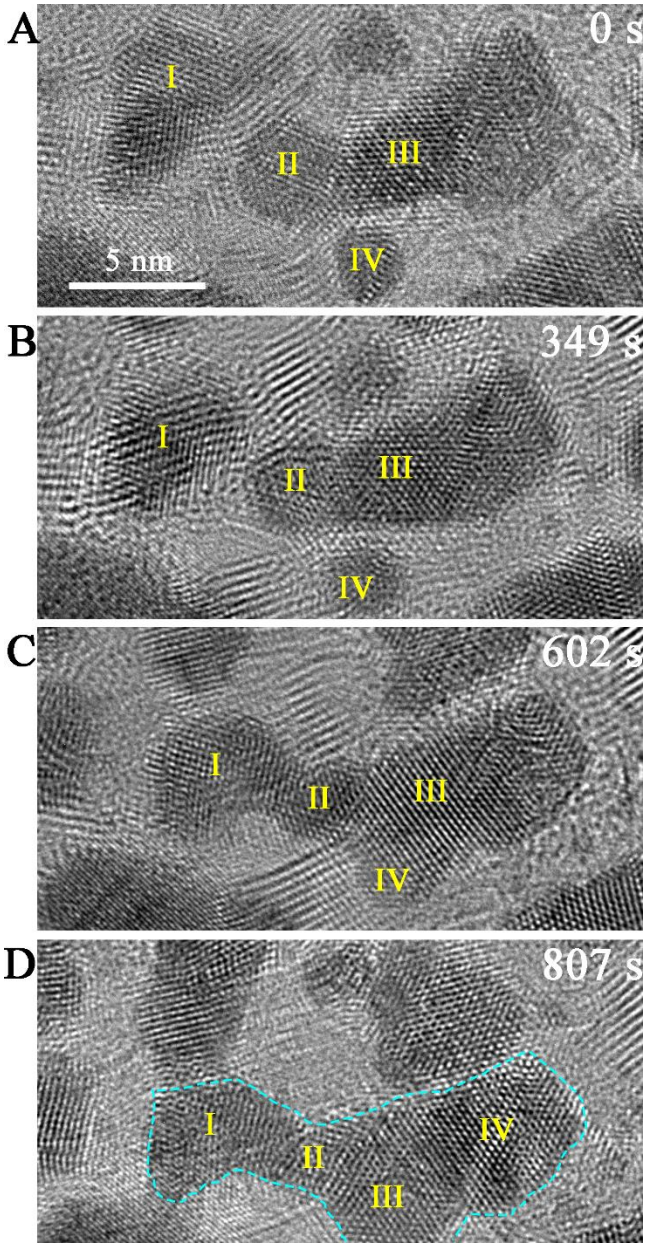

Figure S16. A typical coalescence event of neighboring nuclei (I, II, III, & IV) during crystallization. Time listed for all figures is relative to the first frame. The scale bar in (A) applies to (B - D). The area indicated by the dashed cyan line in (D) corresponds to the final particle shape.

Supplementary Note 1. Reciprocal lattice calculations for SAED & HRTEM analysis

It is known that for a hexagonal lattice, the parameter relationship for the unit cell should obey the following formula: $a=b\neq c$, $\alpha=\beta=90°$, $\gamma=120°$. Based on the as-known crystallographic parameters, the interplanar distance value for certain *(h, k, l)* can be calculated as:

$$g^2=\frac{1}{d^2}=\frac{4}{3a^2}\left(h^2+hk+k^2\right)+\frac{l^2}{c^2}$$

Meanwhile, the angle between the normal to two selected crystal planes (h_1, k_1, l_1) and (h_2, k_2, l_2) can be given by:

$$\cos\Phi=\frac{\frac{4}{3a^2}\left[h_1h_2+k_1k_2+\frac{1}{2}(h_1k_2+h_2k_1)\right]+\frac{l_1l_2}{c^2}}{g_1g_2}$$

In case of tungsten carbide, the theoretical values of typical crystal planes are calculated and summarized in **Table S1**. These results were used in assigning HRTEM/SAED micrographs across this work.

Table S1. Typical reciprocal space parameters calculated from the W_2C structure.

u v w	$h_1\ k_1\ l_1$	$h_2\ k_2\ l_2$	R_2/R_1↑	*Φ (deg)*	D_1 *(ang.)*	D_2 *(ang.)*
0 0 1	0 -1 0	1 0 0	1.000	120.00	4.486	4.486
1 2 1	-1 0 1	1 -1 1	1.000	77.78	3.252	3.252
-1 4 2	0 1 -2	-2 0 -1	1.031	80.24	2.089	2.026
1 1 0	0 0 -1	-1 1 0	1.052	90.00	4.721	4.486
-2 3 1	-1 -1 1	1 0 2	1.087	85.87	2.271	2.089
3 4 2	-2 1 1	0 -1 2	1.087	64.81	2.271	2.089
1 2 3	2 -1 0	1 1 -1	1.141	64.00	2.590	2.271
1 2 2	0 -1 1	2 -1 0	1.256	90.00	3.252	2.590
1 1 1	-1 1 0	0 -1 1	1.379	111.25	4.486	3.252

2 3 1	1 -1 1	2 -1 -1	1.432	77.34	3.252	2.271
2 3 2	-1 0 1	2 -2 1	1.605	91.82	3.252	2.026
1 2 0	0 0 -1	-2 1 0	1.823	90.00	4.721	2.590
1 1 2	-1 1 0	-1 -1 1	1.976	90.00	4.486	2.271
2 2 1	-1 1 0	0 -1 2	2.147	103.46	4.486	2.089
1 1 3	-1 1 0	-2 -1 1	2.811	79.75	4.486	1.596
2 2 3	1 -1 0	1 2 -2	3.258	98.83	4.486	1.377
3 3 2	-1 1 0	-1 -1 3	3.336	90.00	4.486	1.345

* [*u v w*] is the zone axis; Φ is the angle between (h_1, k_1, l_1) and (h_2, k_2, l_2); D_1 and D_2 are the lattice distances of (h_1, k_1, l_1) and (h_2, k_2, l_2) in the real space, respectively.

Table S2. Details of the different W/C heterostructures for MD simulations.

Samples		Lattice constant(Å)	X length (Å)	Y length (Å)	Z length (Å)
Group 1	SC C	2.1	63.0	63.0	18.9
	BCC W	3.16	63.12	63.12	18.96
	Amorphous C		63.0	63.0	18.9
	Amorphous W		63.12	63.12	6.32/9.48/12.64
Group 2	SC C	2.11	73.85	73.85	18.99
	BCC W	3.7	74.0	74.0	22.2
	Amorphous C		73.85	73.85	18.99
	Amorphous W		74.0	74.0	7.4/11.1/14.8
Group 3	SC C	2.1	79.8	79.8	18.9
	BCC W	4.0	80.0	80.0	24.0
	Amorphous C		79.8	79.8	18.9
	Amorphous W		80.0	80.0	8.0/12.0/16.0

Supplementary Movie S1. Dynamics of the spinodal decomposition and the subsequent nucleation processes. The W/C film decomposes into irregular nanoparticles, and then W_2C nucleates within the nanoparticles.

Supplementary Movie S2. Dynamics of the W_2C nanoparticles development process. The irregular W_2C nanostructures show complex behaviors (splitting, coalescing, rearranging, faceting *et al.*) to form faceted nanoparticles.

Supplementary Movie S3. Dynamics of the proposed two-step nucleation pathway of a W/C heterostructure (composed of a 7.4 Å thick amorphous W film and a 19.0 Å thick amorphous C film) *V.S.* annealing time produced by MD simulation. See also **Figure 2** for the representative frames.

References

(1) Xie, D.; Wang, M. P.; Qi, W. H.; Cao, L. F. Thermal Stability of Indium Nanocrystals: A Theoretical Study. *Mater. Chem. Phys.* **2006**, *96*, 418–421.

(2) Mirjalili, M.; Vahdati-Khaki, J. Prediction of Nanoparticles' Size-Dependent Melting Temperature Using Mean Coordination Number Concept. *J. Phys. Chem. Solids* **2008**, *69*, 2116–2123.